Detection and Characterization of Domestic Heat Pumps

Guillaume Le Ray, Morten Herget Christensen, Pierre Pinson
Technical University of Denmark
Centre for Electric Power and Energy
Kgs. Lyngby, Denmark
email:{gleray,mhchris,ppin}@elektro.dtu.dk

***Abstract*—Smart meters allow utilities to gain access to tremendous amount of power consumption data, from which they may improve their knowledge of their customers. In this paper, we propose a method to detect and characterize domestic heat pumps from household electricity consumption data. Appliance detection is not a trivial task, owing to the variability in heat pump load dynamics and to the distortion of their power consumption signature by other appliances. Compared to State-of-the-art methodologies that relies on energy disaggregation with supervised learning and high-resolution data (e.g., 10 seconds), our novel approach uses lower resolution data. Also, it is semi-supervised and relies on a Bayesian framework allowing to continuously learn as new data becomes available. To do so, the overall power consumption signals are decomposed and approximated into a dictionary of boxcar functions using sparse signal approximation to isolate heat pump activity. The learning phase consists then to generate distributions summarizing power consumption, operation time and frequency of heat pump activity summarized as boxcar functions after approximation. During the test phase, those distributions are used as prior to identify boxcar generated by heat pump. Using standard classification performance measure and an application to data from the EcoGrid EU project, the methodology reaches high performance in heat pump detection.**

***Index Terms*—Bayesian framework, energy analytics, heat pump detection, semi-supervised learning.**

I. Introduction

The deployment of two-way communication smart meters and more generally information and communication technologies form the basis of the smart grid. Its aim is to manage and operate the grid in a more effective manner through an optimized integration of Renewable Energy Sources (RES) as well as decentralized generation. The intermittency of RES generation may there be accommodated through the implementation of modern forms of Demand Side Management (DSM), allowing for a paradigm shift with consumption partially following generation [1].

At the same time, large electrical appliances, like heat pumps or electric vehicles or air coolers, are an increasing part of the domestic customers electricity consumption [2]. In a DSM context if equipped with a controller, they can also be an asset for aggregators or Distribution System Operators (DSOs) as they can be used as virtual generator by moving their consumption in time and provide flexibility [3] or services [4], [5] to the grid. Furthermore for marketing purposes it will drastically reduce costs to target customers with these appliances to enroll them in a more energy efficient program or propose a flexibility contract for example [6]. Hence it is strategically important to know at a distribution level which households are equipped with those appliances.

In recent years, an approach called Non Intrusive Load Monitoring (NILM), first described in 1992 by Hart [7], became reality thanks to increasing power consumption data collection and computational power. It consists of disaggregating overall metered power consumption into individual appliances' power consumption. State-of-the-art NILM algorithms require high data resolution (down to the second) and training (supervised) which makes it complicated to implement [8]. From a utility perspective, the only data available are measurement from smart meters, mostly power consumption data, at a resolution from 1 minute to 1 hour. Hence NILM as it is, is not possible to implement at large scale. In a previous work, an unsupervised NILM methodology has been presented which showed performances in the same magnitude as the state-of-the-art NILM algorithm but it proved to perform as well at 1 minute and at 6 seconds (divided by 10 the number of samples) [9]. The methodology relies on a sparse approximation of the signal into a set of boxcar functions selected from an overcomplete dictionary. After clustering the boxcars according to their shape, a community detection algorithm is run to group clusters with strong cross-temporal dependencies that will form the load signature of multilevel appliances.

In this work we propose an application of the framework to a specific use case: the detection of heat pump. Indeed beyond providing feedback to customers, little work has been done to provide specific application of NILM [10]. From the original methodology in [9], the community detection has been removed and a Bayesian framework has been added to generate distribution describing the behavior of heat pumps.

The remaining of the paper is organized as follows: Section II presents the empirical framework; Section III introduces the different elements of the methodology; Section IV reports the results of the methodology on different resolutions and Section V provides conclusions and ideas for future works.

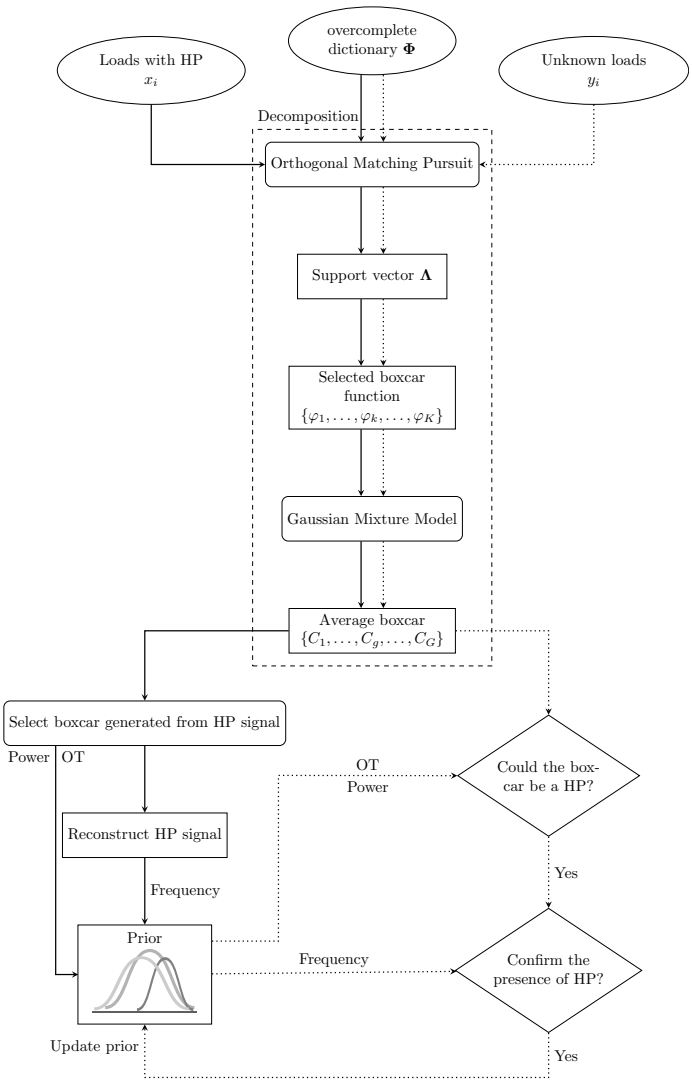

Fig. 1. Algorithm overview.

II. Data Presentation

The data used have been collected during the EcoGrid EU project, which was completed in 2015 [11]. Only a small section of the data collection, corresponding to the coldest period (i.e. where we know the heat pump are active), ranging from the 26th of December 2014 to the 31st of December 2014 is used in this demonstration. The resolution of the data is 5 minutes, which means that the heat pumps when active are easily identified from a plot of the power consumption when active.

A part of the households in the dataset is known to be equipped with heat pump and labelled as such. The other part is unlabelled, which does not mean that households are not equipped with heat pump. Among the households equipped with heat pump, 50 are selected for the training set. The test set consists of 10 households randomly picked among the households labelled with heat pump as well as 65 unlabelled households for a total of 75 households.

III. Methodology

The signal decomposition (dashed box in Figure 1) is a simplified version of the work implemented in [9]. Indeed heat pump's, air cooler's or electric vehicle's charging power consumption Type I appliances (ON/OFF). Hence using the power signal sparse approximation and a clustering is sufficient to isolate heat pump power consumption signal.

The methodology is a semi-supervised approach, with a training step, described in Section III-C, where a prior is learned from a dataset of households labelled as equipped with active heat pump (solid line in Figure 1). The second step, developed in Section III-D, is the heat pump detection of unlabelled households using the prior which is inferred after every iteration (dotted line in Figure 1).

A. Power Signal Sparse Approximation

Signal approximation takes a signal and approximated it as the sum of boxcar function as presented in Figure 2. In practice it takes boxcar functions φ_k subjects to

$$\begin{bmatrix} x^1 \\ x^2 \\ \vdots \\ x^T \end{bmatrix} \approx \begin{bmatrix} \alpha_1 \\ \alpha_2 \\ \vdots \\ \alpha_K \end{bmatrix} \begin{bmatrix} \varphi_1^1 & \varphi_2^1 & \cdots & \varphi_K^1 \\ \varphi_1^2 & \ddots & & \\ \vdots & & \ddots & \vdots \\ \varphi_1^T & & \cdots & \varphi_K^T \end{bmatrix}, \tag{1}$$

with α_k the activation coefficient of boxcar function φ_k, from a dictionary $\mathbf{\Phi} = \{\varphi_k\}_{k=1}^K$ (Figure 1) and generates a sparse support vector $\mathbf{\Lambda}$ with the non-zero elements in $\boldsymbol{\alpha} = [\alpha_1, \ldots, \alpha_k, \ldots, \alpha_K]$ of boxcar function selected to approximate the signal $\mathbf{x}$.

The dictionary, generated beforehand, is said to be overcomplete as the set of basis functions, consisting in all the possible translation-invariant boxcar in the signal, is much larger than the dimension of the input.

The dictionary summarizes what we know about the appliances load behavior and how to approximate it both accurately and in a simple manner. Appliances are mostly of two types, I and II, which have respectively two states (ON/OFF) and many states (OFF and several activation states). The simplest way to approximate such signals is using translation-invariant boxcar functions as building blocks

$$\varphi_{l,w}^t = \frac{1}{\sqrt{w}} \, \Pi_{l-w/2,l+w/2}^t, \tag{2}$$

where l is the boxcar translation and w the width [12]. The boxcar function is made of two Heaviside function as, $\Pi_{a,b}^t = H(t-a) - H(t-b)$, where the $H(\cdot)$ is a Heaviside step function.

Practically, the approach flags changes in power due to an ON/OFF switch or change in state with a fixed or adaptive threshold. The aim is to approximate the power consumption signal so that the internal states fluctuation are removed resulting in simplified the power signal averaged over the activation state (Figure 2).

Iterative processes using a greedy algorithm can be implemented to avoid complexity of a direct sparse approximation,

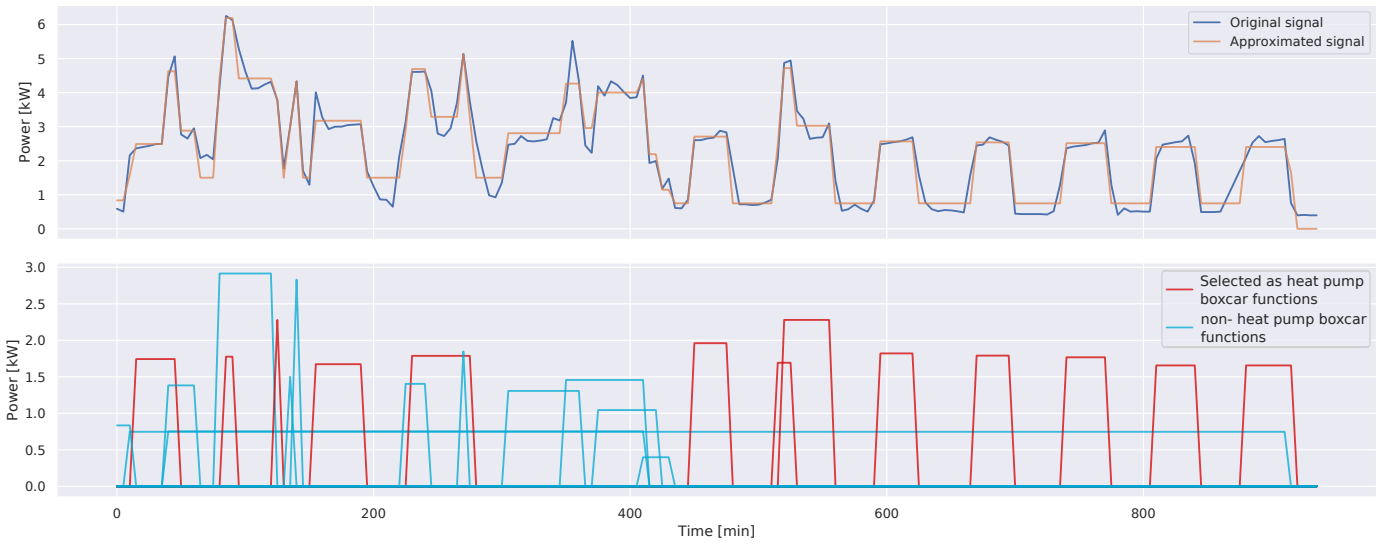

Fig. 2. Raw and approximated power consumption (top) and corresponding boxcar functions of an household equipped with heat pump.

i.e. using combinatorial optimization [13]. At each iteration, a local optimal solution, also close enough to a global one (i.e. overall approximation), is found. The most known greedy algorithm is matching pursuit; it selects a function in the dictionary according to the function contribution in the sparse signal recovery. Orthogonal matching pursuit is an improved version of matching pursuit by updating all the activated coefficients at every iteration in computing the orthogonal projection of the selected functions. Hence it iteratively estimates the coefficients, and discards them when needed. Orthogonal matching pursuit is computationally more expensive but also returns more accurate results.

The orthogonal matching pursuit algorithm starts with the residuals $R^0 = \mathbf{x}$, the coefficient $\alpha^0 = \mathbf{0}$ and $\Lambda^0 = \emptyset$. At each iteration j the residual $R^j = \mathbf{x} - \widehat{\mathbf{x}}^j$ is updated by subtracting $\widehat{\mathbf{x}}^j$ the approximated signal. The next function selected, $\varphi_{k_{max}^{j+1}}$, in the dictionary $\mathbf{\Phi}$ is the one that maximizes

$$k_{max}^{j+1} = \underset{k}{\operatorname{argmax}} \left| R^j \varphi_k^\top \right|_2 \quad \forall k \notin \Lambda^j, \tag{3}$$

the ℓ_2-norm of the inner product $R^j \varphi_k^\top$. At each iteration, a single element $\varphi_{k_{max}^{j+1}}$ is added to the signal recovery $\widehat{\mathbf{x}}^j$ simultaneously updating the sparse support vector

$$\Lambda^{j+1} = \Lambda^j \cup k_{max}^{j+1} \quad \forall k \notin \Lambda^j, \tag{4}$$

The coefficients $\boldsymbol{\alpha}^j$ are then computed as least square

$$\boldsymbol{\alpha}^j = \underset{\boldsymbol{\alpha}}{\operatorname{argmin}} \left\| \mathbf{x} - \boldsymbol{\alpha}_{\Lambda^j} \mathbf{\Phi}_{\Lambda^j} \right\|_2 = \mathbf{\Phi}_{\Lambda^j}^\dagger \mathbf{x}, \tag{5}$$

where $\mathbf{\Phi}_{\Lambda^j}^\dagger$ is the Moore-Penrose pseudo-inverse of $\mathbf{\Phi}_{\Lambda_j}$ the subset of selected boxcars in the dictionary. The last iteration generates the sparse support vector $\Lambda^J = \{k^j\}_{j=1}^J$ restricting the dictionary to $\mathbf{\Phi}_{\Lambda^J}$. The sparse approximated signal can be reconstructed using $\mathbf{x} \approx \boldsymbol{\alpha}_{\Lambda^J} \mathbf{\Phi}_{\Lambda^J}$ (Figure 2).

Concretely the output of the power signal sparse approximation is a set of boxcar functions of different width $\mathbf{w}$ and height $\boldsymbol{\alpha}$ with their location in time approximating the power consumption signal when summed up as showed in Figure 2.

B. Clustering

A direct consequence of the dictionary being overcomplete is that most of the boxcar functions are used only once. However many are displaying similar height α (i.e. power) and width w (i.e. operation time). Indeed they are often generated by the same appliance (e.g. heat pump) and the sparse approximation estimates them differently due to the presence of other appliances or a variation in the load signature. In order to reconstruct the power signal of a heat pump, all the boxcars from the heat pump have to be flagged. It is then a long and tedious task to analyze the boxcar functions one-by-one. To speed up the process, a clustering is implemented on the selected set of boxcar function $\mathbf{\Phi}_\Lambda$ with power amplitude $\boldsymbol{\alpha}$ and operation time $\mathbf{w}$ (see Figure 1).
The clusters may vary differently in amplitude and operation time which means that they have various shape in the 2D space $(\boldsymbol{\alpha}, \mathbf{w})$. Hence Gaussian Mixture Model (GMM) that can form round or ellipsoidal clusters is a suitable algorithm [14]. Each boxcar function φ_k of $\mathbf{\Phi}_\Lambda$ has then coordinates $y_k = (\alpha_k, w_k)$ and $\mathbf{y} = \{y_1, \ldots, y_K\}$. The GMM model of G clusters is then written

$$p(\mathbf{y}) = \sum_{g=1}^{G} \phi_g \, \mathcal{N}(\mathbf{y} \mid \boldsymbol{\mu}_g, \mathbf{\Sigma}_g) \quad \forall g : \phi_g \geq 0, \tag{6}$$

where $\boldsymbol{\mu_g}$ is the mean, $\mathbf{\Sigma}$ is the covariance matrix and ϕ_g is the mixture coefficient of the g^{th} component. The total probability density function sums up to one with $p(\mathbf{y}) \geq 0$ and $\mathcal{N}(\mathbf{y} \mid \boldsymbol{\mu}_g, \mathbf{\Sigma}_g) \geq 0$. It implies that the mixture coefficients ϕ_g must satisfy

$$\sum_{g=1}^{G} \phi_g = 1 \quad \text{and} \quad 0 \leq \phi_g \leq 1. \tag{7}$$

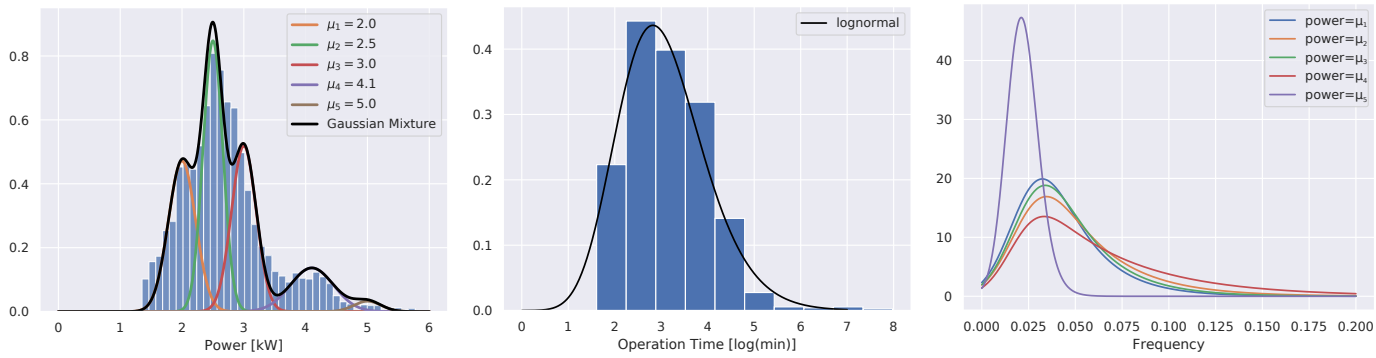

(a) Power consumption priors (b) Duration or operation time prior (c) Frequency of activation prior

Fig. 3. Prior generated during the training phase.

The number of components G is determined empirically, according to how much the dictionary should be reduced. In this specific implementation, $G = 40$ for every household.

C. Training Phase: Prior Definition

The solid line and the left hand side of Figure 1 represent the training phase of the methodology. During the training phase, the subset of households that are equipped with heat pump is processed through signal sparse approximation and clustering. From the approximate signal and the centroids of the clusters, heat pumps' power consumption is visually assessed, hence clusters with the corresponding power consumption are flagged (Figure 1 & 2). Thereafter the power α (height) and the operation time w (width) of each boxcar in the flagged clusters are extracted. The heat pump power consumption signal is then reconstructed with the set of flagged boxcars. The frequency of activation of each heat pump can be computed by differentiating the heat pump consumption signal and counting how many times the differentiated signal is positive over a rolling window of half a days.

Using the empirical distribution of the power, operation time and the frequency, Probability Density Functions (PDF) (Gaussian, Lognormal and Weibull) are then fitted. The best fit for each feature is presented in Figure 3. The power consumption $\boldsymbol{\alpha}$ is actually a Gaussian mixture where the different Gaussian distributions $p(\boldsymbol{\alpha}) = \sum_{p=1}^{P} \phi_p \, \mathcal{N}(\boldsymbol{\alpha} \,|\, \boldsymbol{\mu}_p, \boldsymbol{\sigma}_p^2)$ with $\boldsymbol{\mu}_p = \{2.0, 2.6, 3.0, 4.0, 5.0\}$ corresponds to the average consumptions of each size of heat pump (Figure 3(a)). The operation time is actually transformed using the natural logarithm of the distribution to fit PDFs. Both the Lognormal and the Weibull fit well the empirical distribution as it exhibits a long tail on the high end side. The Lognormal PDF is then chosen as it is simpler to handle (Figure 3(b)). The fit of the frequency is a conditional PDF to each power consumption $\boldsymbol{\mu}_p$. The empirical distributions of the frequency fits a Lognormal PDF as they exhibit also a long tail on the high end side (Figure 3(c)).

The set of three PDFs forms the prior definition of heat pumps' load behavior which can be used to identify the presence of heat pump from the overall electricity consumption of unlabelled households.

D. Test Phase: Heat Pump Detection and Characterization

The heat pump detection phase is presented with a dotted line and the right hand side of Figure 1. As for the learning phase, the overall households' consumption signals are processed through sparse signal approximation and GMM. From the PDFs of the power consumption, the likelihood

$$\mathcal{L}(\mu_p \,|\, \alpha) = f(\alpha \,;\, \mu_p, \sigma_p^2) = \frac{1}{\sigma_p \sqrt{2\pi}} e^{-\frac{1}{2}\left(\frac{\alpha - \mu_p}{\sigma_p}\right)^2} \tag{8}$$

of each centroid power consumption α being sampled from a heat pump with power consumption μ_p is calculated as well as the likelihood of the power consumption not being sampled from a heat pump that follows a lognormal distribution

$$\mathcal{L}(\mu_0 \,|\, \alpha) = f(\alpha \,;\, \mu_0, \sigma_0^2) = \frac{1}{\alpha} \frac{1}{\sigma_0 \sqrt{2\pi}} e^{-\frac{1}{2}\left(\frac{\ln \alpha - \mu_0}{\sigma_0}\right)^2}. \tag{9}$$

The maximum likelihood decoding is obtained by calculating

$$P[\alpha = \mu_p] = \frac{\mathcal{L}(\mu_p \,|\, \alpha)}{\sum_{p=0}^{P} \mathcal{L}(\mu_p \,|\, \alpha)} \tag{10}$$

for each values of μ_p and returns the probability that each centroid is sampled for a specific distribution.

A counting with weighting of the centroids by the number of boxcars they are generated from is done to determine which μ_p has the most often the highest probability. The clusters with the selected μ_p as potential heat pump size are then kept and the likelihood, the maximum likelihood decoding as well as as the counting is then implemented on individual boxcars. The households which have μ_0 as the most probable power consumption are then considered not being a domestic heat pump and thus left aside.

The lognormal PDF fitted on the natural logarithm of the operation time is then used to calculate the likelihood of each boxcar being generated by a heat pump from an operation time perspective. As with the power, the PDF of the natural logarithm of operation times of boxcars not generated by heat pumps is used to calculate the complementary likelihood

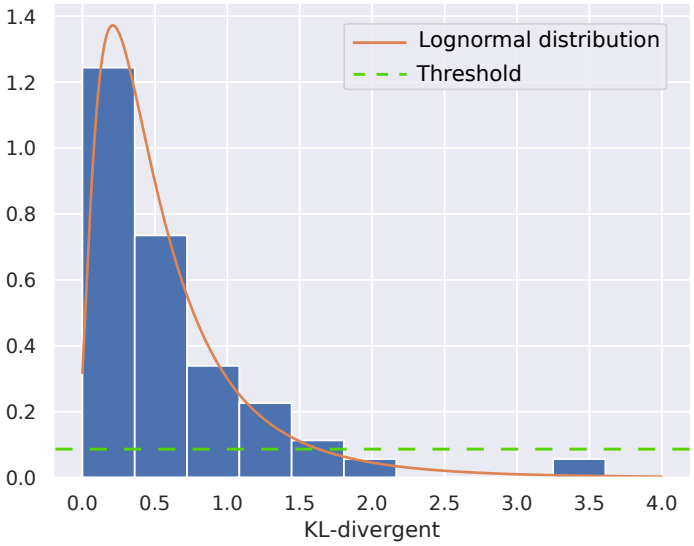

Fig. 4. Distribution of the Kullback-Leibler divergence calculated between the frequency PDF fitted on individual households in the trainning set and the corresponding frequency PDF in Figure 3(c). The orange line is the fitted lognormal PDF and the green dotted line is the threshold under which it is unlikely that a distribution of frequencies is sampled from a heat pump.

of each boxcar not being generated by a heat pump. After decoding of the maximum likelihood, the discrimination of the household possibly equipped with heat pump and the one without is operated by counting which of the options has the most often the hightest probability.

The last step consists of recreating the consumption signal of probable heat pump using the set of boxcars that are likely to be produced by a heat pump. As in Section III-C, the consumption signal is differentiated to calculate, using a rolling window of half a day, the frequencies of activation. The frequency PDF is conditional to the power of the heat pump, μ_p, hence the PDF used to calculate the likelihood of each consumption signal being generated by a heat pump is conditional to its evaluated power consumption μ_p. In this case, the decoding of the maximum likelihood cannot be done as it will require high computing resources to decompose all the signal to calculate the likelihood of frequencies generated by other appliances. Hence, the Kullback-Leibler divergence

$$D_{KL}(P \,||\, Q) = -\sum_i P(i) \ln\left(\frac{P(i)}{Q(i)}\right) \qquad (11)$$

between the conditional PDFs of the frequency generated during the training phase, and each individual heat pump frequency PDF of the training set is calculated. The output, Figure 4, is another lognormal PDF, which allows us to define a threshold of 0.1 under which we assume it's unlikely that the frequency is sampled from a heat pump power consumption signal.

E. Performance Metrics

The performance of our detection algorithm is evaluated using standard classification performance measures, the performance of the prediction is evaluated in comparison to (what we suppose to be) the ground truth.

TABLE I
CONFUSION MATRIX

		Actual	
		Positive	Negative
Predicted	Positive	True Positive (TP)	False Positive (FP)
	Negative	False Negative (FN)	True Negative (TN)
		P	N

From the output of the confusion matrix (Table I), the recall or True Positive Rate (TPR), the precision, also known as Positive Predictive Value (PPV), and the accuracy (ACC)

$$\text{TPR} = \frac{\text{TP}}{\text{TP + FN}} \;,\; \text{PPV} = \frac{\text{TP}}{\text{TP + FP}} \;,\; \text{ACC} = \frac{\text{TP+TN}}{\text{P + N}}$$

are calculated.

IV. RESULTS

The results of the test phase are presented in Table II. The performance measures are calculated at each step of the detection as well as for the overall performance of the algorithm. The results are also presented with the outlook of what we know a priori is the ground truth (left hand side of the table) and after corrections checking for unlabelled heat pump detected and thus considered false positive (right hand side of the table). Indeed, as explained in Section II uncertainties exist in the subset of unlabelled households on the presence of heat pump. Therefore, households' load that seem to be misclassified as equipped with heat pump have to be visually checked. After visual checking of all the false positive but also false negative, three households which were not labelled as equipped with heat pump were displaying patterns that were identified as heat pump and were actually correctly detected. None unlabelled heat pump were placed in the false negative.

TABLE II
PERFORMANCE OF THE DETECTION AT EACH STEP, WITH OR WITHOUT CORRECTING FOR FALSE POSITIVE BEING ACTUAL HEAT PUMP.

	A priori			Corrected		
	TPR	PPV	ACC	TPR	PPV	ACC
Power	0.80	0.11	0.15	0.84	0.16	0.19
Operation Time	1.0	0.23	0.56	1.0	0.30	0.60
Frequency	0.88	0.32	0.21	0.91	0.45	0.35
Overall	0.70	0.31	0.75	0.77	0.46	0.80

The first step of the detection assigns a potential heat pump size to each loads, hence the classification performance is not high and only the TPR is actually relevant as we do not want to discard households labelled with heat pump. Nevertheless two households with heat pump are discarded at this stage of

the detection. They both present consumption which are on the extremity of the range $[1.2, 6.0]$ that we consider possible for domestic heat pump based on the PDFs in Figure 3(a). All the other households discarded at this step have power consumption under 1.5kW which has a low probability for the presence of a heat pump.

From an operation time perspective, the detection assigns well all households with heat pump as having a heat pump. This process is discriminating with a correct accuracy (0.56), without misclassifying households labelled with heat pump (TPR=1.0).

The frequency step is simply refining the classification by reducing the false positive rate as it has the highest PPV of the different steps. It has discarded only one labelled heat pump which presents a relatively high frequency for a heat pump.

The Overall performance of the algorithm is correct in term of detection of the heat pump labelled as such. However the false positives are still relatively high which leads to low PPV performance event after correction. A thorough examination of the set of false positives at the end of the process reveals that it consists of households equipped with large electric heating which in these case have a load behavior similar to heat pump, in terms of amplitude and frequency. Their operation times are in contrary relatively short (5 minutes or less) but they were not discarded as the operation time prior is not strict on the low side of the distribution (see Figure 3(b)). These information are valuable as they help us to update the prior, to improve the performance of the algorithm through inference.

V. Conclusions and Future Works

This paper presents a Bayesian framework to detect domestic heat pumps and characterize their load behaviour. After generating a first definition of heat pumps' load behaviour using PDFs summarizing the range of possible power consumption, operation time and frequency, a first inference is implemented and its performance evaluated. It proved to be performing well despite a small training set resulting in a relatively slack prior definition. The results of this work could be generalized to electric vehicles charging and air coolers which are also large ON/OFF appliances.

The methodology presents already a level of accuracy which could bring valuable insights for targeted marketing strategies regarding efficiency programs or flexibility contract. Indeed, heat pump electric vehicles charging, air coolers are potentially flexible as they are not continuously related to human activities like stoves or light can be. The possibility of knowing where these appliances are geographically placed at a grid distribution level is actually fundamental for efficient DSM and distributed energy generation management. Indeed, the smartness of the grid is not in the meter or in the technology but in the information obtained from processing data and used to take decision. The prior generated could also be used to simulate heat pump power consumption behavior at a population level and understand how the synchronicity of the peak load can affect the grid.

Future works would consist in updating the prior definition, observing its evolution and studying the evolution of the performance of the detection. It would also be interesting to test the detection of electric vehicles charging as the diversity of technologies of chargers makes it more complex.

Acknowledgment

The authors thank EcoGrid EU partners for supporting this work by providing the dataset, as well as the EUDP for funding through the EnergyLab Nordhavn project (EUDP 64015-0055).

References

[1] G. Strbac, "Demand side management: Benefits and challenges," *Energy policy*, vol. 36, no. 12, pp. 4419–4426, 2008.

[2] P. Mancarella, "Mes (multi-energy systems): An overview of concepts and evaluation models," *Energy*, vol. 65, pp. 1–17, 2014.

[3] D. Papadaskalopoulos, G. Strbac, P. Mancarella, M. Aunedi, and V. Stanojevic, "Decentralized participation of flexible demand in electricity marketspart ii: Application with electric vehicles and heat pump systems," *IEEE Transactions on Power Systems*, vol. 28, no. 4, pp. 3667–3674, 2013.

[4] T. Masuta and A. Yokoyama, "Supplementary load frequency control by use of a number of both electric vehicles and heat pump water heaters," *IEEE Transactions on smart grid*, vol. 3, no. 3, pp. 1253–1262, 2012.

[5] W. Kempton and J. Tomić, "Vehicle-to-grid power implementation: From stabilizing the grid to supporting large-scale renewable energy," *Journal of power sources*, vol. 144, no. 1, pp. 280–294, 2005.

[6] H. Fei, Y. Kim, S. Sahu, M. Naphade, S. K. Mamidipalli, and J. Hutchinson, "Heat pump detection from coarse grained smart meter data with positive and unlabeled learning," in *Proceedings of the 19th ACM SIGKDD international conference on Knowledge discovery and data mining*. ACM, 2013, pp. 1330–1338.

[7] G. W. Hart, "Nonintrusive appliance load monitoring," *Proceedings of the IEEE*, vol. 80, no. 12, pp. 1870–1891, 1992.

[8] A. Zoha, A. Gluhak, M. A. Imran, and S. Rajasegarar, "Non-intrusive load monitoring approaches for disaggregated energy sensing: A survey," *Sensors*, vol. 12, no. 12, pp. 16 838–16 866, 2012.

[9] P. Winkler, G. Le Ray, and P. Pinson, "Unsupervised energy disaggregation: From sparse signal approximation to community detection," *IEEE Transaction on Smart Grid*, Submitted.

[10] S. Barker, S. Kalra, D. Irwin, and P. Shenoy, "Nilm redux: The case for emphasizing applications over accuracy," in *NILM-2014 workshop*. Citeseer, 2014.

[11] Y. Ding, S. Pineda, P. Nyeng, J. Østergaard, E. M. Larsen, and Q. Wu, "Real-Time Market Concept Architecture for EcoGrid EU - A Prototype for European Smart Grids," *IEEE Transactions on Smart Grid*, vol. 4, no. 4, pp. 2006–2016, 2013.

[12] S. Arberet and A. Hutter, "Non-intrusive load curve disaggregation using sparse decomposition with a translation-invariant boxcar dictionary," in *Innovative Smart Grid Technologies Conference Europe (ISGT-Europe), 2014 IEEE PES*. IEEE, 2014, pp. 1–6.

[13] L. Daudet, "Audio sparse decompositions in parallel," *IEEE Signal Processing Magazine*, vol. 27, no. 2, pp. 90–96, 2010.

[14] C. M. Bishop, *Pattern Recognition and Machine Learning*. Springer, 2006.